



HAL
open science

Chemical evolution of primordial salts and organic sulfur molecules in the asteroid (162173) Ryugu

Toshihiro Yoshimura, Yoshinori Takano, Hiroshi Naraoka, Toshiki Koga, Daisuke Araoka, Nanako Ogawa, Philippe Schmitt-Kopplin, Norbert Hertkorn, Yasuhiro Oba, Jason Dworkin, et al.

► To cite this version:

Toshihiro Yoshimura, Yoshinori Takano, Hiroshi Naraoka, Toshiki Koga, Daisuke Araoka, et al.. Chemical evolution of primordial salts and organic sulfur molecules in the asteroid (162173) Ryugu. Nature Communications, 2023, 14 (1), 10.1038/s41467-023-40871-0 . hal-04353155

HAL Id: hal-04353155

<https://hal.science/hal-04353155>

Submitted on 19 Dec 2023

HAL is a multi-disciplinary open access archive for the deposit and dissemination of scientific research documents, whether they are published or not. The documents may come from teaching and research institutions in France or abroad, or from public or private research centers.

L'archive ouverte pluridisciplinaire **HAL**, est destinée au dépôt et à la diffusion de documents scientifiques de niveau recherche, publiés ou non, émanant des établissements d'enseignement et de recherche français ou étrangers, des laboratoires publics ou privés.

1 **Chemical evolution of primordial salts and organic sulfur molecules in** 2 **the asteroid (162173) Ryugu**

3
4 Toshihiro Yoshimura^{1*}, Yoshinori Takano^{1*}, Hiroshi Naraoka², Toshiki Koga¹, Daisuke
5 Araoka³, Nanako O. Ogawa¹, Philippe Schmitt-Kopplin^{4,5}, Norbert Hertkorn⁴, Yasuhiro
6 Oba⁶, Jason P. Dworkin⁷, José C. Aponte⁷, Takaaki Yoshikawa⁸, Satoru Tanaka⁹,
7 Naohiko Ohkouchi¹, Minako Hashiguchi¹⁰, Hannah McLain⁷, Eric T. Parker⁷, Saburo
8 Sakai¹, Mihoko Yamaguchi¹¹, Takahiro Suzuki¹¹, Tetsuya Yokoyama¹², Hisayoshi
9 Yurimoto¹³, Tomoki Nakamura¹⁴, Takaaki Noguchi¹⁵, Ryuji Okazaki², Hikaru Yabuta¹⁶,
10 Kanako Sakamoto¹⁷, Toru Yada¹⁷, Masahiro Nishimura¹⁷, Aiko Nakato¹⁷, Akiko
11 Miyazaki¹⁷, Kasumi Yogata¹⁷, Masanao Abe¹⁷, Tatsuaki Okada¹⁷, Tomohiro Usui¹⁷,
12 Makoto Yoshikawa¹⁷, Takanao Saiki¹⁷, Satoshi Tanaka¹⁷, Fuyuto Terui¹⁸, Satoru
13 Nakazawa¹⁷, Sei-ichiro Watanabe¹⁰, Yuichi Tsuda¹⁷, Shogo Tachibana^{17,19}, Hayabusa2-
14 initial-analysis SOM team²⁰

15
16 ¹ Biogeochemistry Research Center (BGC), Japan Agency for Marine-Earth Science and Technology
17 (JAMSTEC), Natsushima 2-15, Yokosuka, Kanagawa 237-0061, Japan.

18 ² Department of Earth and Planetary Sciences, Kyushu University, 744 Motoooka, Nishi-ku, Fukuoka,
19 819-0395, Japan.

20 ³ Geological Survey of Japan (GSJ), National Institute of Advanced Industrial Science and
21 Technology (AIST), 1-1-1 Higashi, Tsukuba, Ibaraki 305-8567, Japan.

22 ⁴ Helmholtz Zentrum München, Analytical BioGeoChemistry, Ingolstaedter Landstrasse 1, 85764
23 Neuherberg, Germany.

24 ⁵ Technische Universität München, Analytische Lebensmittel Chemie, Maximus-von-Forum 2,
25 85354 Freising, Germany.

26 ⁶ Institute of Low Temperature Science (ILTS), Hokkaido University, N19W8 Kita-ku, Sapporo,
27 060-0189, Japan.

28 ⁷ Solar System Exploration Division, NASA Goddard Space Flight Center, Greenbelt, Maryland
29 20771, U.S.A.

30 ⁸ HORIBA Advanced Techno, Co., Ltd., Kisshoin, Minami-ku Kyoto 601-8510, Japan.

31 ⁹ HORIBA Techno Service Co., Ltd. Kisshoin, Minami-ku Kyoto 601-8510, Japan.

32 ¹⁰ Department of Earth and Planetary Sciences, Nagoya University, Nagoya 464-8601, Japan.

33 ¹¹ Thermo Fisher Scientific Inc., 3-9 Moriyacho, Kanagawa-ku, Yokohama-shi, Kanagawa 221-0022,
34 Japan.

35 ¹² Department of Earth and Planetary Sciences, Tokyo Institute of Technology, Ookayama, Meguro,
36 Tokyo 152-8551, Japan.

37 ¹³ Creative Research Institution (CRIS), Hokkaido University, Sapporo, Hokkaido 001-0021, Japan

38 ¹⁴ Department of Earth Science, Tohoku University, Sendai 980-8678, Japan.

- 39 ¹⁵ Department of Earth and Planetary Sciences, Kyoto University, Kyoto 606-8502, Japan.
- 40 ¹⁶ Earth and Planetary Systems Science Program, Hiroshima University, Higashi Hiroshima 739-
41 8526, Japan.
- 42 ¹⁷ Institute of Space and Astro-nautical Science, Japan Aerospace Exploration Agency (ISAS/JAXA),
43 Sagamihara, Kanagawa 229-8510, Japan.
- 44 ¹⁸ Kanagawa Institute of Technology, Atsugi 243-0292, Japan.
- 45 ¹⁹ UTokyo Organization for Planetary and Space Science (UTOPS), University of Tokyo, Bunkyo-ku,
46 Tokyo 113-0033, Japan.
- 47 ²⁰ The Hayabusa2-initial-analysis SOM team: Hiroshi Naraoka, Yoshinori Takano, Jason P. Dworkin,
48 Kenji Hamase, Aogu Furusho, Minako Hashiguchi, Kazuhiko Fukushima, Dan Aoki, José C.
49 Aponte, Eric T. Parker, Daniel P. Glavin, Hannah L. McLain, Jamie E. Elsila, Heather V.
50 Graham, John M. Eiler, Philippe Schmitt-Kopplin, Norbert Hertkorn, Alexander Ruf, Francois-
51 Regis Orthous-Daunay, Cédric Wolters, Junko Isa, Véronique Vuitton, Roland Thissen, Nanako
52 O. Ogawa, Saburo Sakai, Toshihiro Yoshimura, Toshiki Koga, Haruna Sugahara, Naohiko
53 Ohkouchi, Hajime Mita, Yoshihiro Furukawa, Yasuhiro Oba, Yoshito Chikaraishi, Takaaki
54 Yoshikawa, Satoru Tanaka, Daisuke Araoka, Fumie Kabashima, Kosuke Fujishima, Hajime
55 Sato, Kazunori Sasaki, Kuniyuki Kano, Shin-ichiro M. Nomura, Junken Aoki, Tomoya
56 Yamazaki, Yuki Kimura.

57

58 * equal contribution

59

60 Correspondence to T. Yoshimura: e-mail: yoshimurat@jamstec.go.jp, TEL: +81-46-867-9783

61

62

63 **Abstract**

64

65 Samples from the carbonaceous asteroid (162173) Ryugu provide information on the
66 chemical evolution of organic molecules in the early solar system. ~~Here we show the~~
67 ~~element partitioning of the major component ions by~~ sequential extractions of salts,
68 carbonates, and phyllosilicate-bearing fractions ~~revealed the element partitioning of the~~
69 ~~major component ions linked with~~ to reveal primordial brine composition of the
70 primitive asteroid. Sodium is the dominant electrolyte of the salt fraction extract.
71 Anions and NH_4^+ ~~were~~ are more abundant in the salt fraction than in the carbonate and
72 phyllosilicate fractions, with molar concentrations in the order $\text{SO}_4^{2-} > \text{Cl}^- > \text{S}_2\text{O}_3^{2-} >$
73 $\text{NO}_3^- > \text{NH}_4^+$. The salt fraction extracts contained ~~sed~~ anionic soluble sulfur-bearing
74 species such as S_n -polythionic acids ($n < 6$), C_n -alkylsulfonates, alkylthiosulfonates,
75 hydroxyalkylsulfonates, and hydroxyalkylthiosulfonates ($n < 7$). The sulfur-bearing
76 soluble compounds ~~may have driven the molecular evolution of prebiotic organic~~
77 ~~material can be key intermediate species in the~~ transformation of simple organic
78 molecules into hydrophilic, amphiphilic, and refractory S allotropes, ~~which may have~~
79 ~~played an essential role in the molecular evolution of prebiotic organic material.~~

80

81 **Introduction**

82 The Hayabusa2 spacecraft provided the opportunity to investigate the
83 carbonaceous parent body and the astrochemical record of the carbonaceous asteroid
84 (162173) Ryugu¹⁻³. The soluble organic matter (SOM) and soluble ionic compositions
85 of Ryugu have been attributed to prebiotic molecular evolution with unique aqueous
86 alteration effects on the parent asteroid⁴. Furthermore, the characterization of organic-
87 rich carbonaceous chondrites and their classification into groups, such as the Mighei-
88 (CM), Renazzo- (CR), and Ivuna-type (CI) groups, has improved understanding of the
89 origin of water-bearing aqueous alteration minerals and their association with organic
90 molecules. This has provided important insights into the primary chemical profiles and
91 duration of aqueous alteration in the early solar system^{e.g. 5-8}. The chemical composition
92 of the samples recovered from Ryugu has been found to be most similar to that of the CI
93 group⁹.

94 Soluble ions act as bulk electrolytes that stabilize surface charge, and they
95 potentially have a specific structural role in organic and inorganic molecules. In
96 addition, because astrochemically relevant volatile and nonvolatile organic molecules
97 may be present both as salts and in bound forms (i.e., physically trapped or chemically
98 bonded to the matrix), they are less likely to be lost by evaporation from the parent
99 body^{e.g. 10}. Ultra-high-resolution mass spectrometry has revealed that various soluble
100 CHO, CHNO, CHOS, and CHNOS species, as well as organometallic CHO–Mg species,
101 are present in the SOM of meteorites^{11,12}. The overall compositional diversity of organic
102 molecules in Murchison meteorite extracts surpasses the compositional diversity of
103 terrestrial biochemical organic matter¹². The order of molecular compositional diversity
104 of Murchison solvent extracts, CHNOS > CHNO > CHOS > CHO, indicates a
105 significant contribution of sulfur. Furthermore, differences in the distributions of mass
106 peaks between CHOS and CHNOS molecules with average H/C ratios imply divergent
107 formation pathways and the loss of precursor signatures of source CHNO and CHO
108 materials¹²; however, the formation mechanisms of CHOS and CHNOS molecules are
109 not yet fully understood. A recently observed high thermal stability of sulfur-
110 magnesium-carboxylates (CHOSMg) may contribute to survival of organic molecules
111 under harsh extraterrestrial conditions¹³. Soluble ions may contribute to the stabilization
112 of organic matter by forming complexes or by existing as salts; however, basic issues
113 such as the composition and charge balance of ions that leach out with SOM have not
114 yet been investigated. Ryugu samples provide data on the astrochemical history of
115 pristine organic matter and its chemical environment.

116 Initial analysis of organic molecules in samples retrieved from the surface of
117 the C-type asteroid Ryugu has revealed a high molecular diversity of CHNOS
118 species^{4,14-17}. A variety of organic compounds, such as racemic mixtures of

119 proteinogenic and non-proteinogenic amino acids, aliphatic amines, carboxylic acids,
120 polycyclic aromatic hydrocarbons, and nitrogen-containing heterocyclic compounds,
121 has been detected, suggesting that long-term chemical processes caused by aqueous
122 alterations may have contributed to the prebiotic molecular evolution of Ryugu⁴. The
123 addition of sulfur functionalities onto CHNO and CHO precursor molecules might have
124 occurred during interactions mediated by water or during solid-state reactions even
125 under the mild temperature conditions of Ryugu (i.e., fluid alteration at $37 \pm 10^\circ\text{C}$,
126 never heated above $\sim 100^\circ\text{C}$ after aqueous alteration⁹). However, soluble sulfur species
127 available to effect S-functionalization are presently unaccounted for in the primordial
128 formation and molecular evolutionary histories of organosulfur compounds.

129 We report here the distribution patterns of major cations, anions, and sulfur
130 compounds in the salt-, carbonate-, and phyllosilicate-bearing fractions of two surface
131 samples from Ryugu (A0106 from the first touchdown site, and C0107 from the second
132 touchdown site). Soluble sulfur compounds were identified which could have been
133 intermediate reactive species in the primordial organic and inorganic molecular
134 evolution on Ryugu. In addition, sulfur has been proposed to exist in the solar system as
135 allotropes such as S_8 (cyclooctasulfur)¹⁴. These sulfur species are almost impossible to
136 observe via astronomical spectroscopy, but cosmic-ray-driven radiation has recently
137 been proposed as a mechanism for the formation of sulfur allotropes¹⁸. We also discuss
138 the process by which highly reactive sulfur is transformed into a more stable chemical
139 form. Furthermore, we quantify the major soluble components of representative
140 reference carbonaceous meteorites (CI1 Orgueil, C2_{ung} Tarda, and CM2 Aguas Zarcas
141 and Jbilet Winselwan) to compare the distribution of the major soluble components over
142 a range of aqueous alteration.

143

144 **Results**

145 **Total sulfur content and isotopic profiles**

146 The total sulfur content (S, wt%) and sulfur isotopic composition ($\delta^{34}\text{S}$, ‰ vs.
147 Vienna Canyon Diablo Troilite [VCDT]) of the studied Ryugu samples (A0106 and
148 C0107) and of representative carbonaceous meteorites are shown in Fig. 1A. Sulfur
149 abundance differed between A0106 (3.3 ± 0.7 wt%)⁴ and C0107 (5.5 ± 0.7 wt%, $n = 5$;
150 sample weight = 20.6 ± 5.4 μg), implying a heterogeneous distribution of sulfides,
151 either horizontally, between the touchdown 1 and 2 sampling locations, or vertically,
152 between the surface and subsurface samples^{1,19,20} (Supplementary Table 1). The bulk
153 sulfur isotopic compositions of the Ryugu samples, however, indicated a homogenous
154 distribution: $\delta^{34}\text{S} = -3.0\text{‰} \pm 2.3\text{‰}$ for A0106 and $\delta^{34}\text{S} = -1.10\text{‰} \pm 1.62\text{‰}$ ($n = 5$) for
155 C0107.

156

157 Major cations and anions in the Ryugu extracts

158 We quantified the anions and cations present in the hot ultrapure H₂O-,
159 HCOOH-, and HCl-soluble phases of the Ryugu samples (Supplementary Figs. 1–3). In
160 these fractions, salts, carbonates, and phyllosilicates are the primary host solids.
161 Hereafter, the fraction comprising anionic and cationic components extracted by hot
162 ultrapure water is defined as the salt fraction (see the caption of Fig. 1B for the original
163 fraction numbers associated with the different solids⁴). A major cation in the salt
164 fraction of Ryugu is Na⁺, which acts as a primary bulk electrolyte (Figs. 1B and 2). In
165 addition, thiosulfate is found only in H₂O-soluble form. A small amount of NH₄⁺ was
166 also detected in this fraction of Ryugu (0.18 μmol/g for the A0106 salt fraction and
167 <0.02 μmol/g for C0107): Orgueil contains ~200 times as much NH₄⁺ (33.54 μmol/g,
168 see Supplementary Information). Anions were more concentrated in the salt fraction
169 than in the carbonate and phyllosilicate fractions, with molar concentrations in the
170 following order: SO₄²⁻ > Cl⁻ > S₂O₃²⁻ > NO₃⁻ (Supplementary Table 2). Unsurprisingly,
171 the organic fraction of all the samples that was extracted by dichloromethane/methanol
172 (DCM/MeOH) contained fewer ionic solutes because of its low polarity compared to
173 ultrapure H₂O, HCOOH, and HCl.

174

175 Soluble sulfur-containing compounds

176 Thiosulfate accounts for 43% of the total dissolved S in the salt fractions from
177 both A0106 and C0107 (Supplementary Table 2). Polythionates yielded the most intense
178 signals in the ultra-high-resolution mass spectra, and were also detected in the methanol
179 extract⁴ (extract #4, Supplementary Fig. 4). Sulfuric acid accounts for approximately
180 6.3% of the total sulfur in A0106 and C0107; thiosulfate makes up approximately 2.4%
181 of the total sulfur in A0106 and C0107 (Supplementary Table 3).

182 The ion species listed in Supplementary Table 2 were measured by ion
183 chromatography with an electrical conductivity detector. For compounds requiring
184 precise mass, we used ion chromatography high-mass-resolution spectrometry (IC-
185 Orbitrap-MS) to detect a series of anion species in the mass range *m/z* 40–750. Sulfur-
186 bearing species were the main components of the dissolved anions in the Ryugu salt
187 fraction (Fig. 3, Supplementary Fig. 5). In addition to sulfuric and thiosulfuric acid,
188 quantified by IC in conductivity detection mode, homologous molecules of S_{*n*}-
189 polythionic acids (*n* < 6) and C_{*n*}-hydroxyalkylsulfonates (*n* < 7, Appendix) were
190 detected in a Ryugu salt fraction recovered by using an extraction order different from
191 that used for the other salt fractions (extract #5; Supplementary Figs. 1B and 5). The *pH*
192 of the salt fraction (#7-1 in Supplementary Fig. 1B) measured at 24.6°C was weakly
193 acidic, with values of 3.946 ± 0.004 for A0106 and 4.186 ± 0.006 for C0107 during the
194 multi-step scanning (Supplementary Fig. 6).

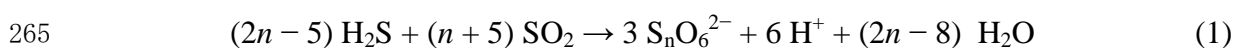
195

196 Discussion

197 Large variations of element abundances were observed between the salt and
198 carbonate fractions of Ryugu (Fig. 1). In the salt fraction, Na^+ accounted for ~90% of
199 the cations (Fig. 2, Supplementary Table 2). Water-chemistry modeling of Ryugu²¹
200 indicated high Na concentrations at low water-to-rock ratios in both fluid and saponite,
201 consistent with the Na-rich composition of the least-altered lithology of Ryugu. The
202 model demonstrates an evolution from Mg–Na–Cl solutions in the early stages of
203 aqueous alteration toward Na–Cl alkaline brines. A striking difference between the
204 modeled fluid and the Ryugu extracts was observed in the profiles of soluble
205 oxygenated sulfur species (Fig. 3). The observed high molecular diversity of S-bearing
206 species provides information about the formation processes of these compounds in
207 Ryugu, as discussed below. The major extractable solutes from the salt and carbonate
208 fractions accounted for 8.0 wt% of solid materials in both A0106 and C0107
209 (Supplementary Table 4); these solutes are considered to have been the major solutes in
210 the Ryugu brine at the onset of salt desiccation. During aqueous alteration, water is
211 consumed by competing hydration and oxidation reactions²². A decrease in the water
212 content would lead to the precipitation of inorganic evaporite minerals. However,
213 inorganic salts (especially Na-, Cl-, and S-bearing salts) are present in only trace
214 amounts or are absent in the Ryugu particles²¹, and in polished sections, carbonates are
215 seen to consist of acid-soluble dolomite [$\text{Ca}, \text{Mg}(\text{CO}_3)_2$], breunnerite [$(\text{Mg}, \text{Fe})\text{CO}_3$],
216 and calcite (CaCO_3), with none of the identified highly soluble Na-containing minerals
217 that may be present in the salt fraction^{9,21}. During aqueous alteration, the major solutes
218 interact with the organic matter, followed by insertion reactions and complexation to
219 SOM. The cation excess (Supplementary Table 4) of our sequential extracts can be
220 considered to represent a balance between SOM (including R-SO_3^- and R-OSO_3^- ; Figs.
221 3, 4), dissolved inorganic carbon species, and dissolved silica. The absence of inorganic
222 sulfate salts has been mineralogically confirmed^{9,21}. Anion adsorption on clay minerals
223 is unlikely to result in large amounts of dissolved sulfur, because saponite has a
224 predominantly negative surface charge²³. Therefore, it is likely that the anions are stored
225 as functional groups of soluble organic matter or their salts. Organosulfur-bearing
226 anions are regarded as credible counterions to Na^+ in the early solar system; aliphatic
227 amines have been proposed to be present as affinity salts in the grains²⁴. We compared
228 the concentrations of soluble ions available for organic reactions with the solvent
229 solubility parameter for hydrophobicity and hydrophilicity of each organic solvent (Fig.
230 5). The increase in the solubility parameter with increasing cation concentrations
231 indicates that the amount and distribution of ions available for organochelates is
232 essentially a function of polarity.

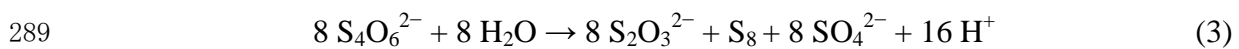
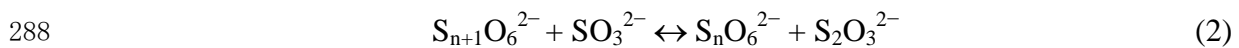
233 Sulfate salts were not detected in Ryugu samples during non-destructive
 234 microscopic observation^{9,21}. Those previous studies concluded that the sulfate veins in
 235 CI meteorites are products of weathering on Earth. In addition, the chemical
 236 composition of the Ryugu particulate matrix was different from that of CI Orgueil, and
 237 sulfate and ferrihydrite were formed from sulfides in CI²⁵. The abundant water-soluble
 238 Mg sulfate veins (epsomite, MgSO₄·7H₂O) in CI Orgueil²⁶ may be a primary
 239 desiccation product in the parent asteroid or represent remobilization and reprecipitation
 240 of soluble sulfates resulting from interaction with the Earth's atmosphere^{27,28}. In the
 241 Mg–Ca–Na+K diagram, the salt fraction of Orgueil plots near the carbonate fraction
 242 (Fig. 2); in addition, these fractions have exceptionally similar δ²⁶Mg values
 243 (Supplementary Fig. 7). The significant enrichment of sulfate in the Orgueil salt fraction
 244 (Fig. 1B) cannot be explained by redistribution of sulfate from the carbonate and
 245 phyllosilicate fractions (Supplementary Table 2); therefore, the observed sulfate
 246 enrichment is considered to derive from the oxidation of FeNi sulfides. Thus, terrestrial
 247 alteration processes such as moisture absorption and the consequent precipitation have
 248 potentially modified CI-type meteorites from their primary composition^{cf. 9}. Magnesium
 249 sulfates are characterized by very high solubility and rapid dissolution in water due to
 250 their hygroscopic nature even under atmospheric conditions; thus, in evaporite
 251 formations on Earth, they are a precipitate indicating very high salinity²⁹. Although the
 252 terrestrial origin of Mg sulfates has been scrutinized from both historical and scientific
 253 perspectives²⁸, the present δ²⁶Mg result for the Orgueil salt fraction indicates that Mg
 254 was redistributed mainly from dolomite. Hence, when Mg-bearing carbonates and
 255 silicate fractions dissolve during terrestrial alteration processes, the Mg should be
 256 partitioned to the salt fraction as a concentrate product. Analysis results of both
 257 elemental concentrations and isotopic ratios support the redistribution of Mg in Orgueil,
 258 confirming the chemically pristine nature of the Ryugu samples⁹.

259 Polythionates are often produced by thiosulfate oxidation, but there are as yet
 260 few constraints on sulfur chemistry and the formation of organosulfur compounds in
 261 carbonaceous chondrite parent bodies³⁰. Polythionates are stable under acidic conditions
 262 (pH ca. 4–5)³¹, consistent with the measured pH of the salt fractions of both A0106 and
 263 C0107 (Supplementary Fig. 6). A generalized reaction for aqueous polythionate
 264 formation has been suggested as follows³² [Eq. 1]:



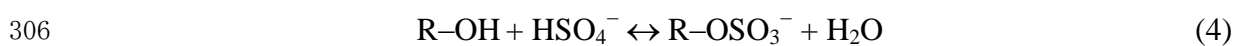
266 Chemical equilibrium modeling of aqueous alteration of the Ryugu parent body,
 267 with mixing of rocks, water containing CO₂ and HCl, and organic matter, yields low
 268 Water/Rock ratios (W/R, ranging from 0.06–0.1 for least-altered to 0.2–0.9 for
 269 extensively altered lithologies) and high Na concentrations in both fluids and the
 270 secondary mineral saponite²¹. Previous comprehensive thermodynamical modeling has

271 demonstrated that, under low W/R conditions, neutralization of the initial HCl-
 272 containing acidic solution results in a Na-rich alkaline fluid in which Na-containing
 273 secondary minerals such as saponite can stably exist²². The Ryugu results suggest the
 274 existence of Mg–Na–Cl-rich solutions in the early stages of aqueous alteration, which
 275 evolved into more reductive, Na–Cl alkaline brines that coexisted with H₂-rich gas
 276 phases²¹. The solutes with high solubility extracted by our hot H₂O method also yield a
 277 Na-rich composition, consistent with the chemical modeling. The most likely possibility
 278 may be that polythionate formation occurred by solid-phase reactions after the escape of
 279 reducing substances such as H₂ and CH₄. Note that the weak *pH* acidity of the eluate of
 280 the salt fraction is based on the ionic balance, which is influenced by both primary
 281 aqueous alteration and subsequent molecular evolution. For example, the Ryugu SOM
 282 contains monocarboxylic acid⁴, which is weakly acidic, and we consider that the *pH* of
 283 the salt fraction also reflects this SOM characteristic. The subsequent elongation of the
 284 polythionate chain and the formation of thiosulfate are governed by the reaction shown
 285 in Eq. 2³³, and then a hydrolysis reaction (Eq. 3 shows that for tetrathionate, but the
 286 reactions for other S_nO₆²⁻ are analogous) produces S₈ as the most stable end product³⁴
 287 (S₈ detection by Aponte et al. 2023¹⁴) [Eq. 3]:



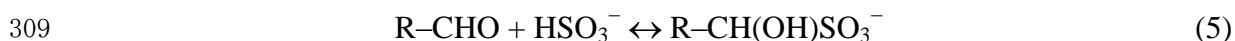
290 These reactions are summarized in Fig. 4, along with the oxidation state of sulfur. In the
 291 particle-phase reaction, high-molecular-weight organosulfur species are formed by
 292 oligomerization under various surface acidities and oxidative conditions³⁵. Furthermore,
 293 the variability of the composition of the organosulfur compounds increases when the
 294 particle-phase acidity is derived from sulfonate groups³⁵. Thus, the presence of soluble
 295 oxygenated sulfur species and the resulting weakly acidic conditions provide an
 296 opportunity for extending the high molecular diversity of extraterrestrial CHNOS and
 297 CHOS molecules. It is also possible that intermediate redox products (e.g., H₂O and
 298 CO₂) produced during the reactions contributed to the water–mineral reaction of
 299 inorganic minerals, consistent with the detection of CO₂-bearing aqueous fluid²¹.

300 Another important property of sulfonate groups is their hydrophilic nature,
 301 which results in the molecular variation trends of hydrophilic molecules observed in the
 302 Murchison meteorite: CHNOS > CHNO > CHOS > CHO¹². Our analysis indicates that
 303 sulfate esters (R–O–SO₃⁻: CH₃SO₄⁻, C₂H₅SO₄⁻, and C₃H₇SO₄⁻) are the most abundant
 304 organosulfur compounds in the salt fraction. These compounds can be formed by sulfate
 305 esterification [Eq. 4]:



307 In addition, hydroxyalkylsulfonic acid can be formed by the the formose reaction of

308 aldehydes quenched by bisulfite³⁶ [Eq. 5]:



310 Organosulfate compounds can be amphiphilic because they are composed of a
311 hydrophilic sulfate group and a hydrophobic hydrocarbon group; thus, they could
312 accumulate on particle surfaces and facilitate inorganic–organic interactions. It is
313 conceivable that such amphiphiles could leave remnant structures, such as the organic
314 nanoglobules observed in carbonaceous meteorites³⁷. Isotopic studies such as those
315 carried out on meteorites³⁸ could clarify the role of this potential mechanism of
316 nanoglobule formation in Ryugu. During further reactions, a variety of soluble
317 organosulfur species are formed (Fig. 4). Alkyl sulfonates produced through the reaction
318 of HCHO and HSO_3^- have been identified in methanol extracts of the Murchison,
319 Tagish Lake, and Allende meteorites³⁷. In the Ryugu methanol extracts, higher-carbon-
320 number species of (hydroxy-)alkylsulfonic/alkylthiosulfonic acid homologs are present
321 (#4, Fig. 3B, Supplementary Fig. 8), as well as sulfide species such as dimethyl
322 disulfide, dimethyl trisulfide, and dimethyl tetrasulfide¹⁴. During self-assembly and
323 transformation of molecules into prebiotic building-blocks, amphiphilic compounds
324 play a key role in encapsulating or integrating insoluble macromolecular matter³⁹ such
325 as mono- and polyaromatic units bonded with O and S and the small aliphatic chains
326 commonly found in carbonaceous chondrites.

327 Finally, the polythionate undergoes decomposition to form a lower-sulfur-
328 number polythionate with elemental sulfur (S_n) [Eq. 3]. Aponte et al. (2023) identified
329 elemental sulfur (S_8) in the methanol extracts from Ryugu samples A0106 and C0107¹⁴.
330 Interestingly, trithionic acid ($\text{H}_2\text{S}_3\text{O}_6$), the least stable polythionic acid whose end
331 products are elemental sulfur and sulfates, at the surface of Ryugu (i.e., sample A0106)
332 is three orders of magnitude less abundant than in sample C0107 (Fig. 4). Surface
333 irradiation might efficiently convert thiosulfates to stable allotropes of S_n .

334 Our analysis of samples from Ryugu has revealed that the abundant soluble
335 sulfur-containing compounds have undergone diverse chemical evolution. The careful
336 curation and lack of opportunities for uncontrolled sample exposure to terrestrial
337 weathering^{19,40} indicate that these compounds are indigenous to Ryugu. Our findings
338 suggest that such transformation reactions could have directly affected the chemical
339 behavior (i.e., the hydrophilic, hydrophobic, and amphiphilic properties) of organic
340 matter. The SOM content of A0106 is less than that of the CM Murchison and
341 comparable to the SOM contents of the unheated CI Ivuna and Orgueil^{4,10,24}. There is a
342 growing interest in the role of minerals and metals in the co-evolution of organic and
343 inorganic matter^{11,41}, and the functionality and abundance of organic matter is specific
344 to mineralogical lithologies⁸. Furthermore, a sample of the carbonaceous asteroid
345 (101955) Bennu is scheduled to be returned in 2023 by the OSIRIS-REx mission.

346 During investigation of Bennu, large veins of calcite, dolomite–breunnerite, and
347 magnesite, presumably formed by aqueous alteration processes, were detected⁴². Future
348 work is expected to verify whether differences in water content and thermal history
349 result in a variety of soluble amphibolic compounds being produced during S-bearing
350 molecular evolution.

351

Methods

Samples and sequential chemical extraction

Samples A0106 and C0107 from Ryugu, and material from the Orgueil, Tarda, Aguas Zarcas, and Jbilet Winselwan meteorites, were studied. The samples were collected at the first touchdown site (A0106) and the second touchdown site (C0107) on the asteroid Ryugu^{1,2}; C0107 contains subsurface samples from the artificially made impact crater⁴³.

Sample weights used for chemical extraction treatments #7-1 to #10 in [Supplementary Fig. 1B](#) were 17.15 mg of A0106, 17.36 mg of C0107, and 17.91 mg of Orgueil meteorite (CI type, from National Museum of Denmark). A sequential extraction was performed on these samples using 600 μL of each of the solvents in the order hot H_2O (#7-1), dichloromethane and methanol (#8), HCOOH (#9), and HCl (#10). The samples sealed in a vacuum were first extracted with #7-1 hot H_2O , weighed immediately after vial opening, and reacted with N_2 gas-purged ultrapure water (Tamapure AA100, Tama Chemical) for 20 h at 105°C in a flame-sealed ampoule with the headspace also purged with N_2 gas. The reaction tube was centrifuged at $13,150 \times g$ for 8 min, opened, and the supernatant was recovered. Dichloromethane (DCM, PCB analysis grade, FUJIFILM Wako Pure Chemical Corporation) and methanol (MeOH, QToFMS analysis grade, Fujifilm Wako pure chemical corporation) were then mixed at a volume ratio of 1:1. The DCM/MeOH extraction (#8) was carried out in an ultrasonic bath (Branson, CPX1800-J) at room temperature for 15 min, and the supernatant was recovered after centrifugation at $9,660 \times g$ for 5 min. Next, $>99\%$ HCOOH (#9, Fujifilm Wako pure chemical corporation) was reacted overnight at room temperature. Finally, a 15-min sonication with 20% HCl (#10, Tamapure AA100, Tama Chemical) at room temperature was performed to complete the extraction of soluble substances. The #9 and #10 fractions were centrifuged under the same conditions as ultrapure water.

Note that the amounts of major cations and anions in each fraction are divided by the initial weights of the starting solid materials used for sequential leaching (in $\mu\text{mol/g}$, [Figs. 1, 3, 5](#)). The percentages of clay mineral and carbonate standards dissolved in the HCOOH and HCl are shown in [Supplementary Table 5](#). Samples from Tarda (15.76 mg), Aguas Zarcas (15.51 mg), and Jbilet Winselwan (14.90 mg) were also subjected to the same extraction experiments for comparison, but only the HCOOH and HCl fractions could be used in this study because they were preferentially used for the analysis of other soluble organic matter. The results for these meteorites are also shown in [Supplementary Table 6](#). This method was previously applied to carbonaceous chondrites such as Murchison as a rehearsal analysis for the Hayabusa2 project, and the concentrations of dissolved constituents in the HCOOH and HCl fractions have been reported⁴⁴.

The other chemical extraction step using organic solvents and ultrapure water is shown in [Supplementary Fig. 1B](#). Sample weights used for #2 to #5 were 17.15 mg of A0106, 17.36 mg of C0107, and 17.56 mg of Orgueil. These samples were subjected to sequential extraction with organic solvents in the order hexane (#2), dichloromethane (#3), and methanol (#4). At each step, the extract was sonicated for 15 min, after which the supernatant was recovered. At the end of the organic solvent extraction, the fractions were extracted with ultrapure water (#5) at room temperature, but only the Orgueil results could be used for this study.

Ion chromatography

After the extraction processes, the anion and cation concentrations of each fraction were measured by ion chromatography (IC), using the Metrohm 930 Compact IC Flex system (Metrohm AG, Herisau, Switzerland). For cations, the samples were eluted through a Metrohm Metrosep C6-250/4.0 column with 8 mM ultrapure HNO₃ (TAMAPURE AA-100, Tama Chemical, Kawasaki, Japan) at a flow rate of 0.9 mL·min⁻¹. Anions were measured with a Metrohm Metrosep A Supp4-250/4.0 column with a chemical suppressor module. The mobile phase consisted of a mixture of 1.8 mM Na₂CO₃ and 1.7 mM NaHCO₃ (Kanto Chemical, Tokyo, Japan) at a flow rate of 0.9 mL·min⁻¹. A chemical suppressor module (Metrohm MSM) was used to decrease the background conductivity of the eluent and to transform the analytes into free anions. The column temperature was set at 35°C throughout the analysis. Detection of cations and anions was accomplished by measuring electrical conductivity.

Ion chromatography/Mass spectrometry

The distribution of anions in the Ryugu extracts was analyzed by using a Dionex ICS-6000 IC system (Thermo Fisher Scientific Inc., Waltham, USA) equipped with an Orbitrap Exploris 480 mass spectrometer (Thermo Fisher Scientific Inc., Waltham, USA). For the IC separation, a Dionex IonPac[®] AS11-HC analytical column (2 × 250 mm, Thermo Fisher Scientific Inc., Waltham, USA) with a guard column was used at 35°C. The mobile phase was KOH at a constant flow rate of 0.25 mL·min⁻¹. The KOH gradient program was 1.0 mM KOH from 0 to 1 min, which was increased to 50.0 mM KOH from 1 to 40 min and held there until 64 min, after which it was decreased to 1.0 mM KOH from 64 to 65 min and held there until 75 min. A conductivity detector combined with an AERS suppressor (Thermo Fisher Scientific Inc., Waltham, USA) was utilized to cross-check the detection of anions by the subsequent mass spectrometry.

The Orbitrap mass spectrometer was equipped with an electrospray ionization (ESI) source and operated in negative ion mode. The flow rates of nitrogen gas for desolvation were set to 40 arbitrary units (Arb) of the sheath gas, 5 Arb for the auxiliary

gas, and 0 Arb for the sweep gas. The ion transfer capillary temperature and ESI spray voltage were set to 320°C and 2.5 kV, respectively. Full scan mass spectra were acquired over a mass range of m/z 50 to 750 with a mass resolution of 120,000 (at full-width-half-maximum for m/z 200). Most ions were detected in the deprotonated form, $[M-H]^-$. The full scan measurements exhibited a general mass accuracy of less than 1 ppm, defined as $[(\text{measured } m/z) - (\text{calculated } m/z)]/(\text{calculated } m/z) \times 10^6$ (ppm). An exclusion list composed of the two largest background peaks, m/z 112.9856 (corresponding to CF_3COO^-) and m/z 68.9958 (corresponding to CF_3^-) was implemented with a mass width of ± 10 ppm to decrease the background signal.

Inductively coupled plasma mass spectrometry

Trace-element concentrations were measured by quadrupole inductively coupled plasma mass spectrometry (ICP-MS, iCAP Qc, Thermo Fisher Scientific Inc., Waltham, USA). A 0.3 M HNO_3 solution was added to each vial to dilute the samples. The HNO_3 used in this study was a commercially supplied high-purity TAMAPURE AA-100 reagent (Tama Chemical, Kawasaki, Japan). We added internal standards (Be, Sc, Y, and In) to the HNO_3 to correct for the instrumental drift.

For the Mg isotope analysis, each extract was dried down, and then re-dissolved in 8 mM HNO_3 . Samples were purified by an IC Metrohm 930 Compact IC Flex system coupled to an Agilent 1260 Infinity II Bio-Inert analytical-scale fraction collector system (Agilent Technologies, Santa Clara, USA) set in a class-1000 clean hood^{45,46}. For complete separation of cations, the samples were eluted through a Metrohm Metrosep C6-250/4.0 column with 8 mM ultrapure HNO_3 at a flow rate of 0.9 $mL \cdot min^{-1}$. Magnesium isotope ratios were measured by a multiple collector (MC) ICP-MS Neptune plus (Thermo Fisher Scientific Inc., Waltham, USA). We performed Mg isotope analysis with a high-sensitivity X-skimmer cone. Sample solutions were introduced with a PFA nebulizer (MicroFlow, $\sim 50 \mu L \cdot min^{-1}$, ESI, Omaha, USA) attached to a quartz dual-cyclonic spray chamber in free aspiration mode. The beam intensity for the 100 ppb solutions was approximately 5.0 V for ^{24}Mg . After initial uptake of the solutions, a single analysis consisted of 40 cycles with an integration time of 4 s per cycle. The background signal intensities were measured with a 0.3 M ultrapure HNO_3 solution for 1 cycle with an integration time of 30 s per cycle.

The isotopic data are expressed as per mil (‰) deviations relative to the DSM-3 standard. The Mg isotope ratio was defined as follows:

$$\delta^{26}Mg = \{ (^{26}Mg/^{24}Mg)_{\text{sample}} / (^{26}Mg/^{24}Mg)_{\text{DSM-3}} - 1 \} \times 1000 \quad (6)$$

pH measurement

After recovering the supernatant by centrifugation during the sequential extraction⁴, we performed *pH* measurements of the hot water fraction (#7-1 for A0106 and C0107) at 24.6°C (within $\pm 0.1^\circ\text{C}$ at ambient atmosphere) by using a LAQUA F-73 instrument (HORIBA Advanced Techno Co., Ltd., Kyoto, Japan) with a *pH* electrode (model 0040-10D), with an instrument repeatability of within ± 0.001 of the *pH* value. In this *pH* measurement process, the small recovered supernatant water fraction (<10 μL) was measured without any dilution. Prior to the measurement, a three-point calibration was performed with phosphate standard solutions of *pH* 4.005 and 6.865 (both at $\sim 25^\circ\text{C}$) and a tetraborate standard solution of *pH* 9.18 (Kanto Chemical Co. Inc) ([Supplementary Fig. 6](#)).

Data Availability

Source data for figures are provided with the paper and available from the corresponding author. The Hayabusa2 project is releasing raw data on the properties of the asteroid Ryugu from the Hayabusa2 Science Data Archives (DARTS, <https://www.darts.isas.jaxa.jp/planet/project/hayabusa2/>). We declare that all these database publications are compliant with ISAS data policies (<https://www.isas.jaxa.jp/en/researchers/data-policy/>).

Code Availability

N/A

References

1. Tachibana, S. et al. Pebbles and sand on asteroid (162173) Ryugu: In situ observation and particles returned to Earth. *Science* **375**, 1011–1016 (2022).
2. Yada, T. et al. Preliminary analysis of the Hayabusa2 samples returned from C-type asteroid Ryugu. *Nat. Astron.* **6**, 214–220 (2022).
3. Pilorget, C. et al. First compositional analysis of Ryugu samples by the MicrOmega hyperspectral microscope. *Nat. Astron.* **6**, 221–225 (2022).
4. Naraoka, H. et al. Soluble organic molecules in samples of the carbonaceous asteroid (162173) Ryugu. *Science* **379**, abn9033(2023a).
5. Ehrenfreund, P., Glavin, D. P., Botta, O., Cooper, G. & Bada, J.L. Extraterrestrial amino acids in Orgueil and Ivuna: Tracing the parent body of CI type carbonaceous chondrites. *Proc. Natl. Acad. Sci. USA* **98**, 2138–2141 (2001).
6. Gounelle, M. & Zolensky, M. E. The Orgueil meteorite: 150 years of history. *Meteorit. Planet. Sci.* **49**, 1769–1794 (2014).
7. Takir, D. et al. Nature and degree of aqueous alteration in CM and CI carbonaceous chondrites. *Meteorit. Planet. Sci.* **48**, 1618–1637 (2013).
8. Schmitt-Kopplin, P. et al. Complex carbonaceous matter in Tissint martian meteorites give insights into the diversity of organic geochemistry on Mars. *Sci. Adv.* **9**, eadd6439 (2023).
9. Yokoyama, T. et al. Samples returned from the asteroid Ryugu are similar to Ivuna-type carbonaceous meteorites. *Science* **379**, eabn7850 (2023).
10. Glavin, D. P. et al. The origin and evolution of organic matter in carbonaceous chondrites and links to their parent bodies. in *Primitive meteorites and asteroids*. (ed. Abreu, N.) 205–271 (Elsevier, 2018).
11. Ruf, A. et al. Previously unknown class of metalorganic compounds revealed in meteorites. *Proc. Natl. Acad. Sci. USA* **114**, 2819–2824 (2017).
12. Schmitt-Kopplin, P. et al. High molecular diversity of extraterrestrial organic matter

- in Murchison meteorite revealed 40 years after its fall. *Proc. Natl. Acad. Sci. USA* **107**, 2763–2768 (2010).
13. Matzka, M. et al. Thermal History of Asteroid Parent Bodies Is Reflected in Their Metalorganic Chemistry. *Astrophys. J. Lett.* **915**, L7 (2021).
 14. Aponte, J. C. et al. PAHs, hydrocarbons, and dimethylsulfides in Asteroid Ryugu samples A0106 and C0107 and the Orgueil (CI1) meteorite. *Earth Planets Space* **75**, 28 (2023).
 15. Parker, E. T. et al. Extraterrestrial Amino Acids and Amines Identified in Asteroid Ryugu Samples Returned by the Hayabusa2 Mission. *Geochim. Cosmochim. Acta* **347**, 42–57 (2023).
 16. Hashiguchi, M. et al. The spatial distribution of soluble organic matter and its relationship to minerals in the asteroid (162173) Ryugu. *Earth Planets Space* **75**, 73 (2023).
 17. Oba, Y. et al. Uracil in the carbonaceous asteroid (162173) Ryugu. *Nat. Commun.* **14**, 1292 (2023).
 18. Shingledecker, C. N. et al. Efficient production of S₈ in interstellar ices: The effects of cosmic-ray-driven radiation chemistry and nondiffusive bulk reactions. *Astrophys. J.* **888**, 52 (2020).
 19. Okazaki, R. et al. First asteroid gas sample delivered by the Hayabusa2 mission: A treasure box from Ryugu. *Sci. Adv.* **8**, eabo7239 (2022).
 20. Okazaki, R. et al. Noble gases and nitrogen in samples of asteroid Ryugu record its volatile sources and recent surface evolution. *Science* **379**, eabo0431 (2023).
 21. Nakamura, T. et al. Formation and evolution of carbonaceous asteroid Ryugu: Direct evidence from returned samples. *Science* **379**, eabn8671 (2023).
 22. Zolotov, M. Y. Aqueous fluid composition in CI chondritic materials: Chemical equilibrium assessments in closed systems. *Icarus* **220**, 713–729 (2012).
 23. Shirozu, H. *Introduction to Clay Mineralogy: Fundamentals for Clay Science*. (Asakura Publishing Co. Ltd, 2010).
 24. Aponte, J. C., Dworkin, J. P. & Elsila, J. E. Indigenous aliphatic amines in the aqueously altered Orgueil meteorite. *Meteorit. Planet. Sci.* **50**, 1733–1749 (2015).
 25. Nakato, A. et al. Ryugu particles found outside the Hayabusa2 sample container. *Geochem. J.* **56**, 197–222 (2022).
 26. DuFresne, E. R. & Anders, E. On the chemical evolution of the carbonaceous chondrites. *Geochim. Cosmochim. Acta* **26**, 1085–1114 (1962).
 27. Brearley, A. J. The action of water. in *Meteorites and the early solar system II* (eds. Laretta, D. S., & McSween, H. Y.) 587–624 (University of Arizona Press, 2006).

28. Gounelle, M. & Zolensky, M. E. A terrestrial origin for sulfate veins in CII chondrites. *Meteorit. Planet. Sci.* **36**, 1321–1329 (2001).
29. Yoshimura, T. et al. An X-ray spectroscopic perspective on Messinian evaporite from Sicily: Sedimentary fabrics, element distributions, and chemical environments of S and Mg. *Geochem. Geophys. Geosys.* **17**, 1383–1400 (2016).
30. Ruf, A. et al. Sulfur ion irradiation experiments simulating space weathering of Solar System body surfaces-Organosulfur compound formation. *Astron. Astrophys.* **655**, A74 (2021).
31. Pan, C., Lv, F., Kégl, T., Horváth, A. K. & Gao, Q. Kinetics and Mechanism of the Concurrent Reactions of Hexathionate with S (IV) and thiosulfate in a slightly acidic medium. *J. Phys. Chem. A* **123**, 5418–5427 (2019).
32. Spatolisano, E. et al. Polythionic acids in the Wackenroder reaction. *ACS Omega* **6**, 26140–26149 (2021).
33. Druschel, G. K., Hamers, R. J. & Banfield, J. F. Kinetics and mechanism of polythionate oxidation to sulfate at low pH by O₂ and Fe³⁺. *Geochim. Cosmochim. Acta* **67**, 4457–4469 (2003).
34. Kanao, T. et al. Reaction mechanism of tetrathionate hydrolysis based on the crystal structure of tetrathionate hydrolase from *Acidithiobacillus ferrooxidans*. *Protein Sci.* **30**, 328–338 (2021).
35. Surratt, J. D. et al. Organosulfate formation in biogenic secondary organic aerosol. *J. Phys. Chem. A* **112**, 8345–8378 (2008).
36. Naraoka, H., Hashiguchi, M. & Okazaki, R. Soluble Sulfur-Bearing Organic Compounds in Carbonaceous Meteorites: Implication for Chemical Evolution in Primitive Asteroid. *ACS Earth Space Chem.* **7**, 41–48 (2023b).
37. Nakamura-Messenger, K., Messenger, S., Keller, L. P., Clemett, S. J. & Zolensky, M. E. Organic globules in the Tagish Lake meteorite: Remnants of the protosolar disk. *Science* **314**, 1439–1442 (2006).
38. De Gregorio, B. T. et al. Isotopic and chemical variation of organic nanoglobules in primitive meteorites. *Meteorit. Planet. Sci.* **48**, 904–928 (2013).
39. Ehrenfreund, P., Rasmussen, S., Cleaves, J. & Chen, L. Experimentally tracing the key steps in the origin of life: The aromatic world. *Astrobiology* **6**, 490–520 (2006).
40. Sakamoto, K. et al. Environmental assessment in the prelaunch phase of Hayabusa2 for safety declaration of returned samples from the asteroid (162173) Ryugu: Background monitoring and risk management during development of the sampler system. *Earth Planets Space* **74**, 90 (2022).
41. Smith, K. E., House, C. H., Arevalo, R. D., Dworkin, J. P. & Callahan, M. P.

- Organometallic compounds as carriers of extraterrestrial cyanide in primitive meteorites. *Nat. Commun.* **10**, Article number: 2777 (2019).
42. Kaplan, H. et al. Bright carbonate veins on asteroid (101955) Bennu: Implications for aqueous alteration history. *Science* **370**, eabc3557 (2020).
 43. Nishiizumi, K. et al. Exposure conditions of samples collected on Ryugu's two touchdown sites determined by cosmogenic nuclides ^{10}Be and ^{26}Al . *53rd Lunar and Planetary Science Conference*, #1777 (2022).
 44. Yoshimura, T. et al. Major and trace element composition in acid-soluble extracts of Murchison and Yamato meteorites. *51st Annual Lunar and Planetary Science Conference*, #2326 (2020).
 45. Yoshimura, T. et al. Lithium, magnesium and sulfur purification from seawater using an ion chromatograph with a fraction collector system for stable isotope measurements. *J. Chromatogr. A* **1531**, 157–162 (2018).
 46. Araoka, D. & Yoshimura, T. Rapid Purification of Alkali and Alkaline-earth Elements for Isotope Analysis ($\delta^7\text{Li}$, $\delta^{26}\text{Mg}$, $^{87}\text{Sr}/^{86}\text{Sr}$, and $\delta^{88}\text{Sr}$) of Rock Samples Using Borate Fusion Followed by Ion Chromatography with a Fraction Collector System. *Anal. Sci.* **35**, 751–757 (2019).
 47. Alexander, C. M. O. D. et al. Sulfur abundances and isotopic compositions in bulk carbonaceous chondrites and insoluble organic material: Clues to elemental and isotopic fractionations of volatile chalcophiles. *Meteorit. Planet. Sci.* **57**, 334–351 (2022).
 48. Lodders, K. Relative atomic solar system abundances, mass fractions, and atomic masses of the elements and their isotopes, composition of the solar photosphere, and compositions of the major chondritic meteorite groups. *Space Sci. Rev.* **217**, 44 (2021).
 49. Williamson, M. A. & Rimstidt, J. D. Correlation between structure and thermodynamic properties of aqueous sulfur species. *Geochim. Cosmochim. Acta* **56**, 3867–3880 (1992).
 50. Palumbo, M. E., Geballe, T. R. & Tielens, A. G. Solid carbonyl sulfide (OCS) in dense molecular clouds. *Astrophys. J.* **479**, 839 (1997).
 51. Rohrschneider, L. Solvent characterization by gas-liquid partition coefficients of selected solutes. *Anal. Chem.* **45**, 1241–1247 (1973).

Acknowledgments

The Hayabusa2 project was led by ISAS (Institute of Space and Astronautical Science)/JAXA (Japan Aerospace Exploration Agency) in collaboration with DLR (German Space Center) and CNES (French Space Center), and supported by NASA

(National Aeronautics and Space Administration) and ASA (Australian Space Agency). We thank the members of the Astromaterials Science Research Group (ASRG) at ISAS, and the Hayabusa2 curation team for conducting the sampling and quality control management. We express our deep appreciation for the constructive and insightful comments from Dr. E. Quirico. We also thank Y. Nakanishi of Thermo Fisher Scientific Inc. for support of the chemical assessment and the molecular-specific identification by mass spectrometry; Y. Yoshikawa of JAMSTEC for laboratory assistance; Mr. Kumazoe of Kyushu University for solvent extraction of the Tarda, Aguas Zarcas, and Jbilet Winselwan meteorites; Y. Kobayashi of Metrohm Japan for technical support with the ion chromatography; and Dr. Y. Tamenori for advice on the chemical species of sulfur. Preliminary reports based on the current results were presented at the Lunar and Planetary Science Conference (LPSC) in 2020 and 2022. This research was partly supported by the Japan Society for the Promotion of Science (JSPS) under KAKENHI grant numbers 21H01204 (TYoshimura), 21H04501&21H05414 (YO), 21J00504 (TK), 21KK0062 (YT), and 20H00202 (HN). JPD and JCA are grateful to NASA for support of the Consortium for Hayabusa2 Analysis of Organic Solubles.

Author Contributions

TYoshimura, YTakano, HN, and JPD conceived the study. HN and YTakano conducted the sequential extraction and distributed the SOM samples. TYoshimura conducted IC analysis. DA and TYoshimura conducted the ICP analysis and the evaluation of the Mg isotopic composition. HN, YO, TK, MY, and TS conducted the Orbitrap analysis. YTakano, TYoshikawa, and STanaka performed the small-scale aqueous analysis of *pH* with authentic standards. NOO and NO performed small-scale elemental analysis of sulfur and isotopic composition, and provided interpretation of the sulfur chemistry. MH, HM, and EP supported the work flow on sequential extraction of reference sample processes with HN and YTakano. TYokoyama, HY, and STachibana provided the interpretation of asteroidal chemistry. HN, YTakano, and JPD designed the implementation of the SOM scheme prior to the initial analysis (until ~31 May 2022). All authors contributed to the data analysis and manuscript revision, and read and approved the submitted version.

Competing interests

The authors declare that they have no competing interests.

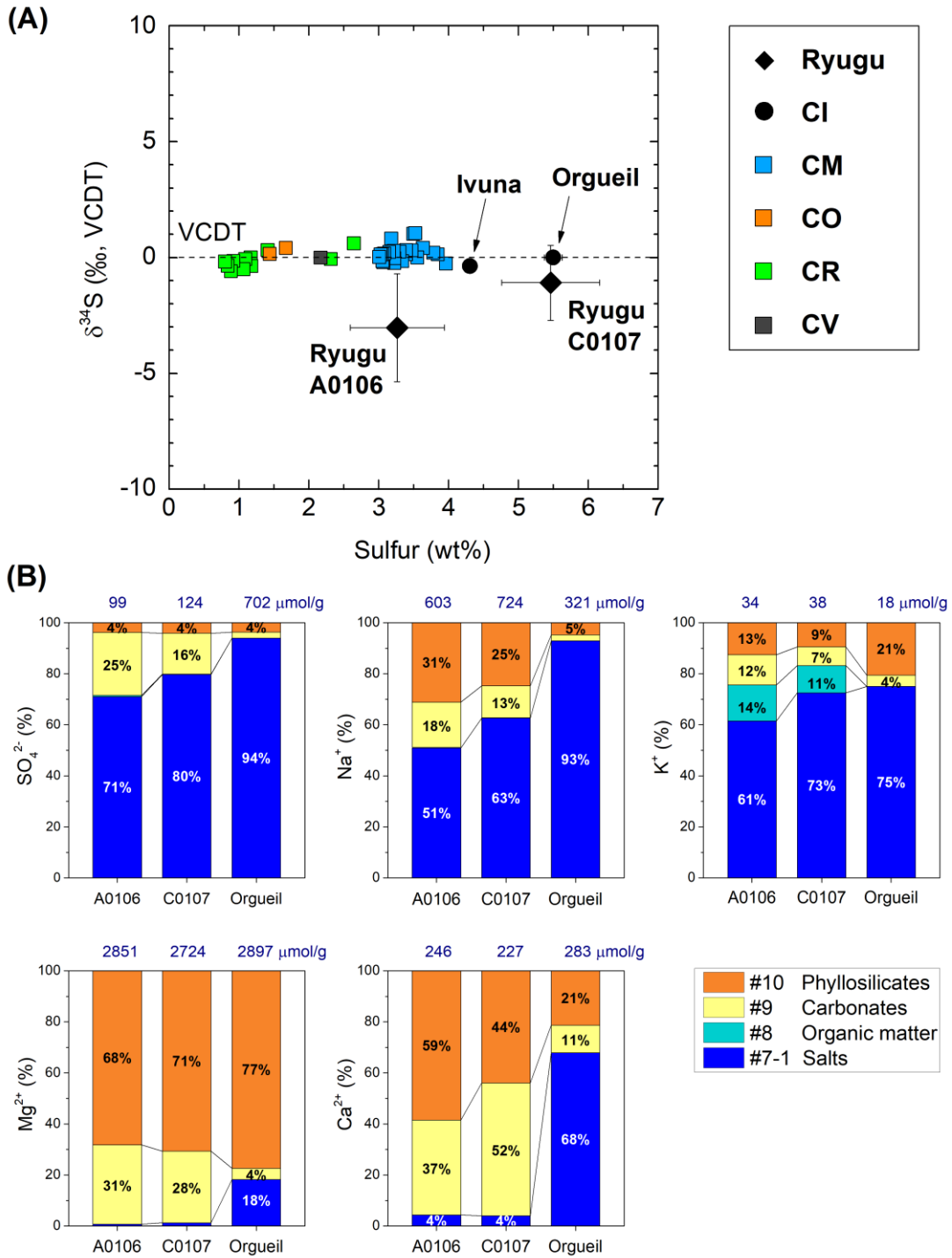


Fig. 1 Element compositions of the Ryugu samples.

(A) Total sulfur content (wt%) and isotopic profiles of the Ryugu samples (A0106, C0107) and of representative carbonaceous groups (CI, CM, CO, CR, and CV). Sulfur (S, wt%) and $\delta^{34}\text{S}$ (‰ vs. VCDT) values are from the literature^{4,17,47} and references therein.

Error bars are one standard deviation (1SD) values of multiple particles.

(B) Relative amounts of sulfate, sodium, potassium, magnesium, and calcium in

sequential solvent extracts of the samples collected at the first touchdown site (A0106) and the second touchdown site (C0107) on the asteroid Ryugu ([Supplementary Fig. 1](#)), and in a sample from Orgueil (values less than 3% were omitted). C0107 may contain subsurface samples from ejecta associated with the artificially made impact crater. We used fine-grained samples and carried out the sequential solvent extraction in a clean room⁴ ([Supplementary Fig. 1](#)). We measured evaporitic salts (via #7-1 hot water extraction, see IDs in [Supplementary Fig. 1](#) and Naraoka et al. 2023a⁴); ions bound to soluble organic matter (via #8 dichloromethane and methanol, **DCM+MeOH**); exchangeable ions and highly soluble minerals such as carbonates (via #9 formic acid, **HCOOH**); and clays and residual soluble minerals (via #10 hydrochloric acid, **HCl**). Navy numbers are the sum of extractable solute contents for each solute.

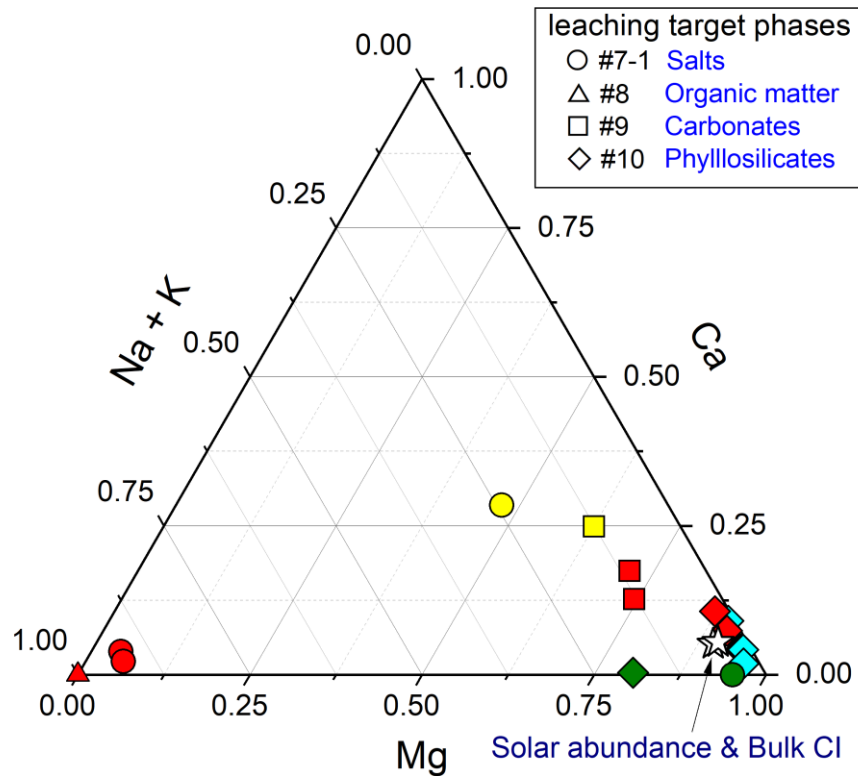


Fig. 2 Ternary diagram illustrating the molar proportions of Mg, Ca, and Na+K in the sequential extracts.

Samples include Ryugu A0106 and C0107 (red), Orgueil (yellow), Tarda, Aguas Zarcas, Jbilet Winselwan (blue), and serpentine (olive), with the bulk compositions of CI chondrite and solar abundance (stars) also plotted for reference⁴⁸. The types of solvents and the main target phases of the leaching experiments are documented in [Supplementary Fig. 1B](#).

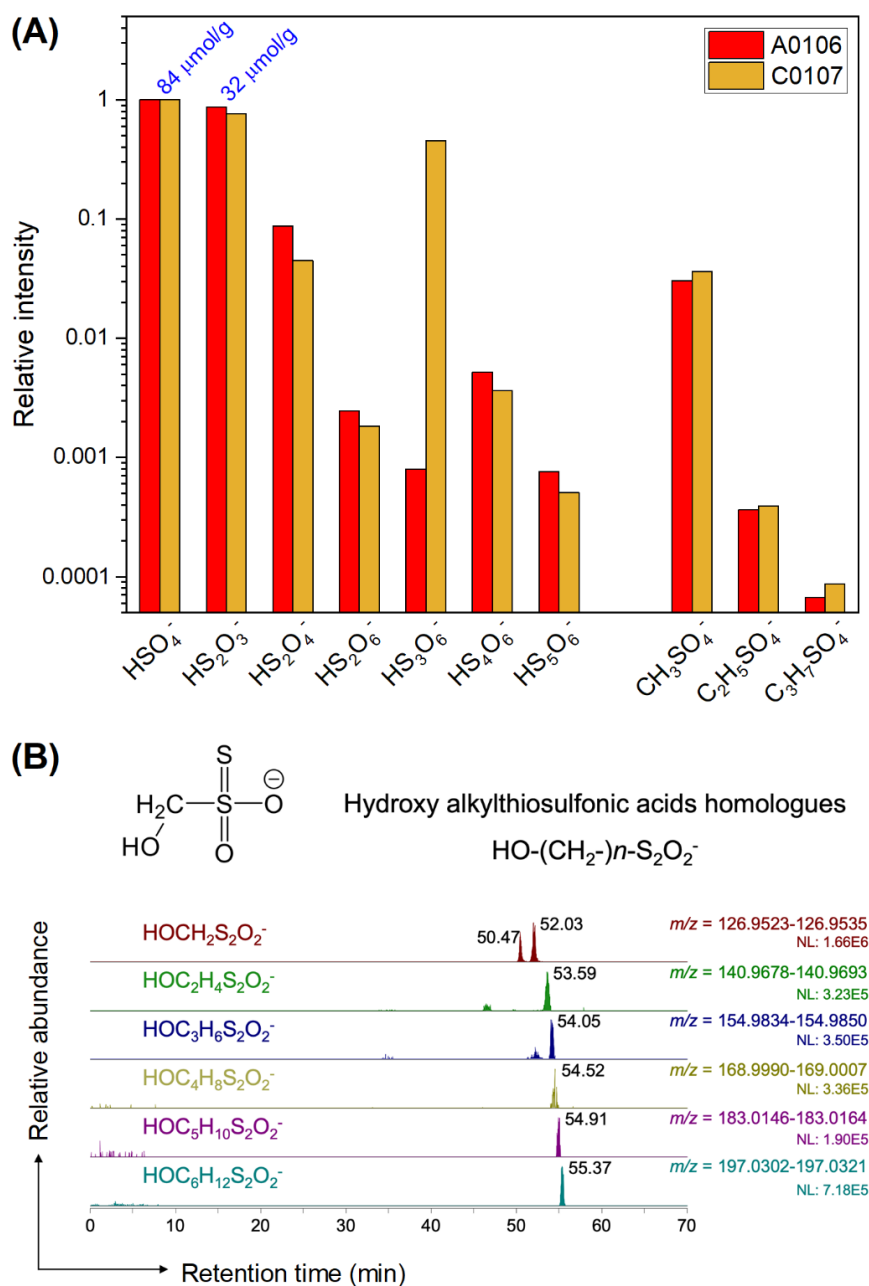


Fig. 3 Anionic soluble sulfur-bearing species.

(A) Relative intensity of major anion species detected by ion chromatography / Orbitrap mass spectrometry (IC/Orbitrap MS) of the water extracts of A0106 and C0107 (#5, [Supplementary Fig. 1B](#)). The intensities are normalized to sulfuric acids and shown on a logarithmic scale. Average sulfate and thiosulfate concentrations of A0106 and C0107 quantified by conductivity detection of ion chromatography analysis are shown above the bars (blue). (B) Representative nano-flow LC/Orbitrap MS chromatograms of water-extractable (#5) organic sulfur homologs. Here we show hydroxy alkylthiosulfonic acid $\text{HO}-(\text{CH}_2)_n-\text{S}_2\text{O}_2^-$ obtained from Ryugu sample A0106. Other organosulfur compounds are shown in [Supplementary Figs. 4 and 8](#).

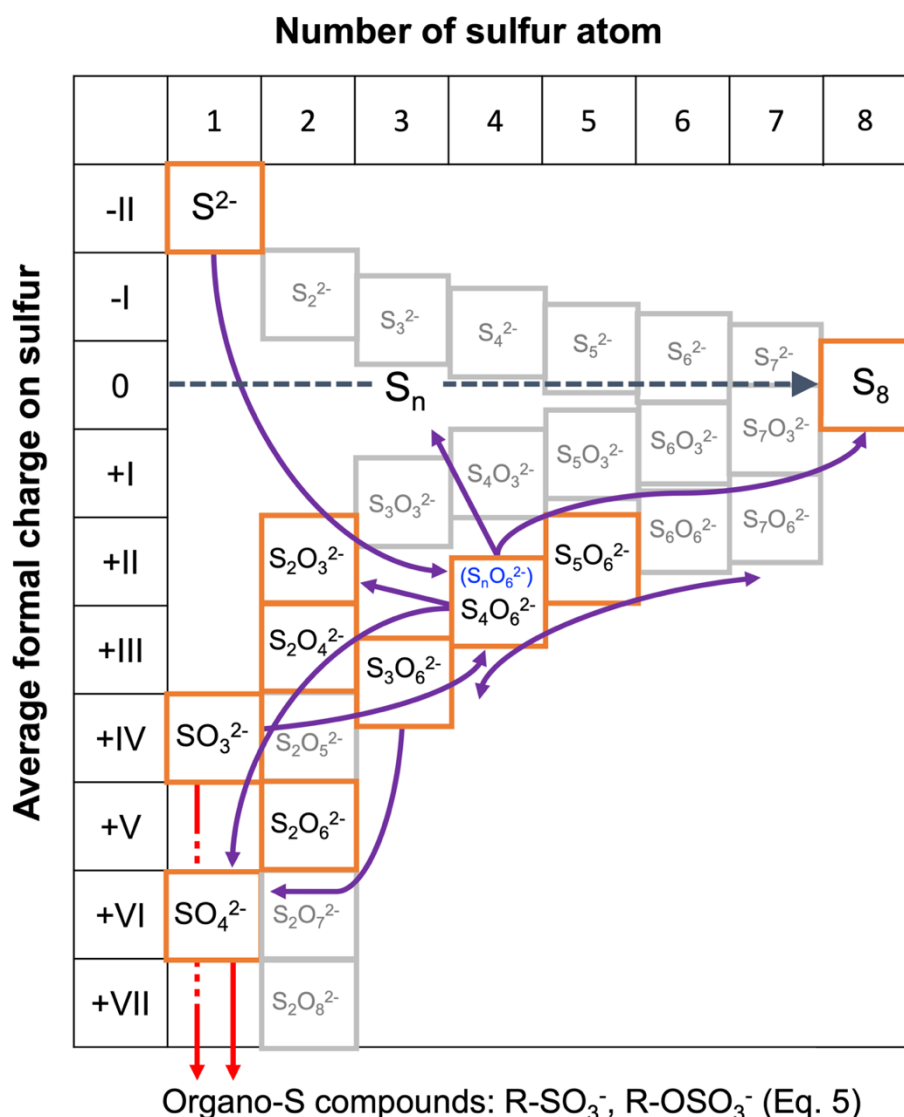


Fig. 4 Reactions along with the oxidation state of sulfur.

Sulfur species and reaction pathways described by Eqs. 1–4 (after Williamson and Rimstidt, 1992)⁴⁹. Two dominant species of organosulfur compounds (R–SO₃⁻ and R–OSO₃⁻) were reported previously³⁶ and are documented in this study. The red line shows the reaction path from inorganic ions to these sulfur-containing organics such as esterification (Eq. 4). The purple line shows the reaction path of sulfur allotropes stabilizing to S₈. Sulfur species detected by our ion chromatography and mass spectrometry analyses are shown in the orange squares. Note that organosulfur compounds with various alkyl side chains have been detected^{4,14} (Fig. 3, Supplementary Fig. 8). For Eq. 1, the presence of SO₂ has been suggested by spectroscopic observations⁵⁰, and both H₂S and SO₂ are generally involved in astrochemical models¹⁸. See also Supplementary Tables 1, 3 and their references for sulfur abundance in the Ryugu sample.

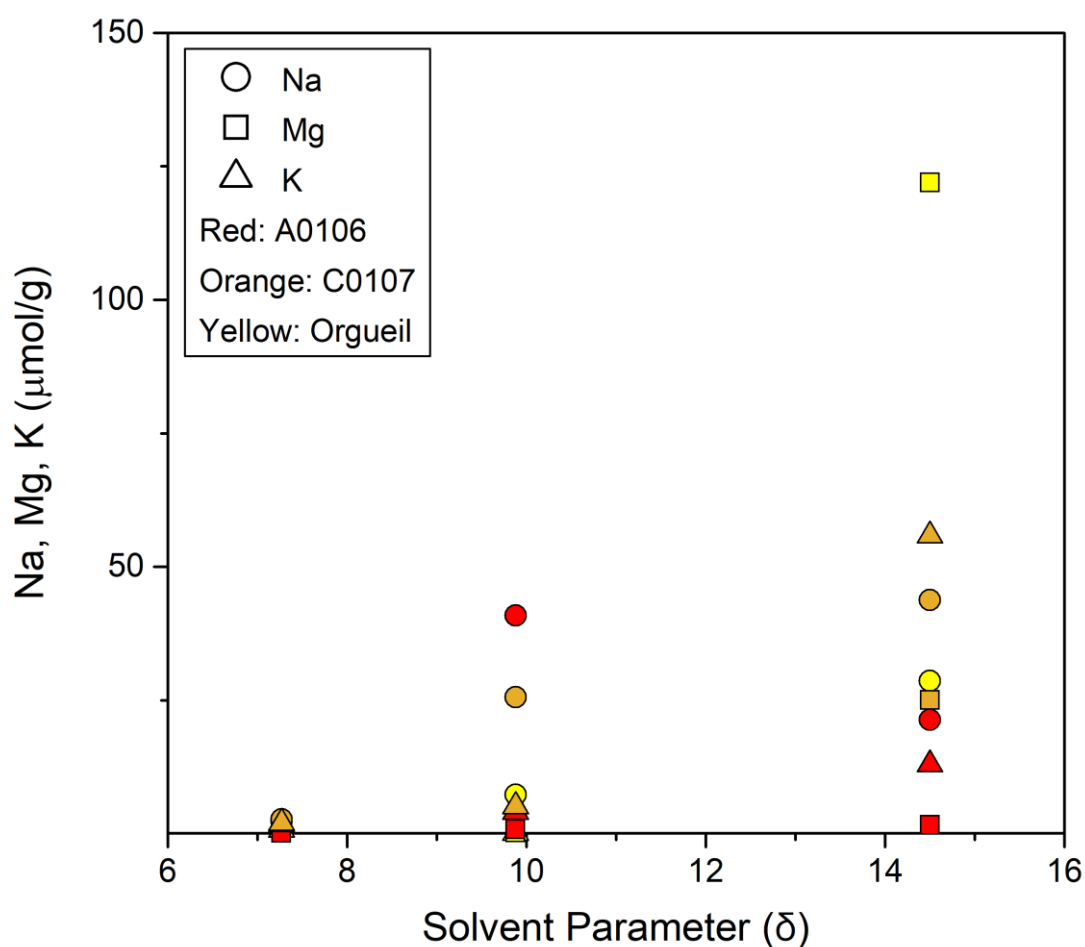


Fig. 5 Sodium (Na), magnesium (Mg), and potassium (K) concentrations in sequential organic solvent extracts vs. solvent solubility parameters (δ)⁵¹.

The solutes were extracted sequentially from lower to higher δ values⁴; hexane ($\delta = 7.3$), dichloromethane ($\delta = 9.9$), and methanol ($\delta = 14.5$). For reference, the δ value of water is 23.5.